Published in final edited form as:

Brain Res. 2018 September 01; 1694: 129–139. doi:10.1016/j.brainres.2018.05.022.

Glycosylation of Cblns attenuates their receptor binding

Yongqi Rong, **Parmil K. Bansal**, **Peng Wei**, **Hong Guo**, **Kristen Correia**, **Jennifer Parris**, and **James I. Morgan**

Department of Developmental Neurobiology, St. Jude Children's Research Hospital, Memphis, Tennessee 38105

Abstract

Cbln1 is the prototype of a family (Cbln1–Cbln4) of secreted glycoproteins and is essential for normal synapse structure and function in cerebellum by bridging presynaptic Nrxn to postsynaptic Grid2. Here we report the effects of glycosylation on the *in vitro* receptor binding properties of Cblns. Cbln1, 2 and 4 harbor two N-linked glycosylation sites, one at the N-terminus is in a region implicated in Nrxn binding and the second is in the C1q domain, a region involved in Grid2 binding. Mutation (asparagine to glutamine) of the N-terminal site, increased neurexin binding whereas mutation of the C1q site markedly increased Grid2 binding. These mutations did not influence subunit composition of Cbln trimeric complexes (mediated through the C1q domain) nor their assembly into hexamers (mediated by the N-terminal region). Therefore, glycosylation likely masks the receptor binding interfaces of Cblns. As Cbln4 has undetectable Grid2 binding *in vitro* we assessed whether transgenic expression of wild type Cbln4 or its glycosylation mutants rescued the Cbln1-null phenotype *in vivo*. Cbln4 partially rescued and both glycosylation mutants completely rescued ataxia in cbln1-null mice. Thus Cbln4 has intrinsic Grid2 binding that is attenuated by glycosylation, and glycosylation mutants exhibit gain of function *in vivo*.

Graphical Abstract

Address correspondence: James I. Morgan, Department of Developmental Neurobiology, St. Jude Children's Research Hospital, 262 Danny Thomas Place, Memphis, TN 38105, USA, Phone: 901-595-2256, Fax: 901-595-3143, jim.morgan@stjude.org.

Conflict of interest

The authors declare no conflicts of interest.

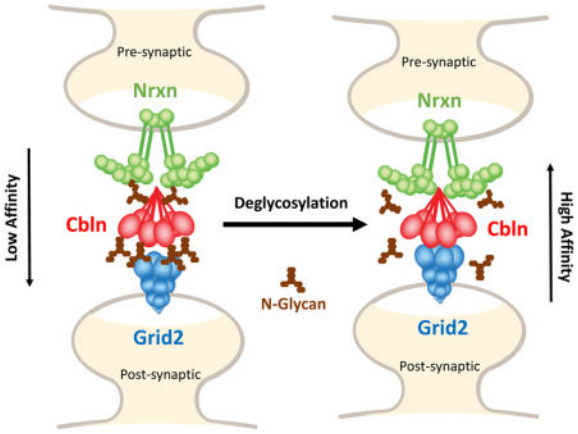

Keywords

glycosylation; transgenic; locomotor activity; S4 domain

1. Introduction

Cbln1 is a member of the C1q/TNF superfamily of proteins (Urade et al., 1991; Bao et al., 2005) and its genetic elimination in mice leads to ataxia due to a loss of synaptic connectivity between cerebellar granule neurons and Purkinje cells (Hirai et al., 2005). Cbln1and its three immediate family members, Cbln2–Cbln4 are secreted as hexameric complexes composed of a dimer of trimers, wherein the C1q domain in the C-terminal half of the protein mediates trimer assembly and a cysteine motif near the N-terminus supports dimerization of trimers via intermolecular disulfide bonding (Bao et al., 2005). Functionally, Cbln1 hexamers behave as bivalent ligands that participate in a trans-synaptic complex that bridges presynaptic Neurexins in granule neurons to post-synaptic Grid2 in Purkinje neurons (Matsuda et al., 2010; Uemura et al., 2010; Elegheert et al., 2016; Cheng et al., 2016). Structural studies have revealed that the N-terminal region of Cbln1 is involved in Nrxn binding whereas Grid2 binding is largely mediated by the C1q domain (Elegheert et al., 2016; Cheng et al., 2016).

Besides their hexameric configuration another cardinal feature of the Cblns is the presence of two conserved N-linked glycosylation sites. One is at the N-terminus, the region implicated in Nrxn binding (Elegheert et al., 2016; Cheng et al., 2016) and dimerization (Bao et al., 2005) and the second is in the C1q domain, the region that mediates both Grid2 binding (Elegheert et al., 2016; Cheng et al., 2016; Zhong et al., 2017) and trimerization of Cbln protomers (Bao et al., 2005). In several C1q/TNF superfamily members, such as complement component C1q (Ritchie et al., 2002) and the cytokine TNFα glycosylation influences biological activity (Koyama et al., 1992). As the glycosylation sites in Cblns are located in the regions implicated in receptor interactions and subunit assembly we addressed the questions of whether glycosylation of the Cblns affected their receptor binding properties or influenced the structure and composition of their complexes. We also sought to assess whether glycosylation contributed to the unique binding of Cbln4 to deleted in colon cancer

(DCC) (Wei et al., 2012) or influenced the dependence of Cbln binding on the presence of the S4 splice region in neurexins. We demonstrate that glycosylation of Cblns markedly and selectively attenuates their receptor binding *in vitro* without altering the subunit composition or stoichiometry of Cbln complexes. Furthermore, ectopically expressed Cbln4 glycosylation mutants *in vivo* are more potent than wild type Cbln4 in rescuing ataxia in Cbln1-null mice. These gain-of-function molecules can be valuable tools in dissection the burgeoning examples of extra-cerebellar functions of Cblns.

2. Results

The Cblns are glycosylated at asparagine residues: Cbln1 N23, N79; Cbln2 N53, N110; Cbln3 N82; Cbln4 N26, N85. One glycosylation site is at the N-terminus (Cbln3 lacks this site) [Fig. 1a], whereas the second is in the αA helix within the C1q domain (Elegheert et al., 2016) [Fig. 1a]. Since Cbln3 is not secreted (Bao et al., 2005), we tested monoglycosylation mutants of Cbln1, Cbln2 and Cbln4 for secretion. All single mutants were secreted [Fig. 1b]. Furthermore PNGase F digestion of WT or monoglycosylation mutants generated an ~20 kDa band, corresponding to the calculated mass of the non-glycosylated proteins [Fig. 1b]. Untreated Cbln2-N53Q, Cbln4-N26Q and Cbln4-N85Q display an additional weak upper band approximately the same size as the untreated wildtype forms [Fig. 1b]. These bands disappear upon PNGase F treatment [Fig. 1b]. These bands may represent a very minor population of Cbln proteins with higher mass glycan chains, although their true identity is unknown and are not seen in double glycosylation site mutants [Fig. 1b].

Monoglycosylation mutants were of intermediate size compared to WT or PNGase digested proteins. Double glycosylation site mutants secrete poorly and have masses indistinguishable from PNGase F-treated Cbln and are PNGase F insensitive [Fig. 1b]. These data establish that Cbln1, Cbln2 and Cbln4 harbor two functional N-linked glycosylation sites [Fig. 1b].

To determine whether glycosylation of Cblns affects their receptor binding properties, we compared the binding of WT Cbln1, Cbln2, Cbln4 and their monoglycosylated mutants to Grid1, Grid2, Nrxn1β, Nrxn3β, and DCC. Compared with mock transfection, Cbln1 bound to Grid2, Nrxn1β, and Nrxn3β but not to DCC [Fig. 2a]. $Cbln1^{N23Q}$ and more prominently $Cbln1^{N79Q}$ had greater Grid1 and Grid2 binding activity than WT Cbln1 [Fig. 2a]. When corrected for input, both glycosylation mutants also exhibited significantly increased Nrxn binding [Fig. 2a]. Neither WT nor Cbln1 mutants bound to DCC. [Fig. 2a]. Cbln2 bound to Nrxn1β and Nrxn3β, had very weak Grid2 binding and undetectable Grid1 or DCC binding [Fig. 2b]. $Cbln2^{N53Q}$ had elevated Nrxn1β and Nrxn3β binding and marginally increased Grid2 binding [Fig. 2b]. $Cbln2^{N110Q}$ had marked binding to Grid2 but Nrxn3β binding was unaffected [Fig. 2b]. Neither WT nor Cbln2 mutants bound to DCC [Fig. 2b]. Cbln4 bound to Nrxn1β and DCC but had undetectable Grid1, Grid2 and Nrxn3β binding [Fig. 2c]. Binding of $Cbln4^{N26Q}$ to Nrxn1β and Nrxn3β was much greater than WT Cbln4. $Cbln4^{N26Q}$ also bound Grid1 and Grid2, and its binding to DCC was also significantly higher than WT. Compared to WT Cbln4, $Cbln4^{N85Q}$ showed an increase in binding to Nrxn1β and Nrxn3β, but showed a dramatic increase in Grid2 binding [Fig. 2c]. In general, elimination of N-

terminal glycosylation sites enhances Nrxn binding whereas elimination of the C1q sites markedly enhances Grid2 binding. The data also suggest that Cbln4 does have weak intrinsic Grid2 binding in vitro that is below the detection limit of the assay.

Cbln1 and Cbln4 interact with Nrxns via a 30 amino acid long splice segment (so-called S4 region) (Joo et al., 2011; Wei et al., 2012). We investigated whether the monoglycosylation mutants retained their dependence on the S4 domain. Neither WT nor monoglycosylation mutants of Cbln1 [Fig. 3a], Cbln2 [Fig. 3b] or Cbln4 [Fig. 3c] bound with S4-deleted (ΔS4) variants of Nrxn1β or Nrxn3β.

DCC belongs to a family of related receptors implicated in developmental processes (Mehlen et al., 1998; Jiang et al., 2003; Mehlen et al., 2007; Castets et al., 2012). We showed Cbln4 associates with DCC (Wei et al., 2012) and a subsequent report (Haddick et al., 2014) also observed neogenin binding. Given the increased binding of monoglycosylated Cbln4, we examined their interaction with all five DCC family members. WT Cbln4 only bound to DCC. However, $Cbln4^{N26Q}$ and $Cbln4^{N85Q}$ also bound to neogenin (Neo1) (p=0.045; p=0.028, respectively) [Fig. 3d], supporting the results of Haddick et al., 2014, but did not bind the other DCC family members, Igdcc3, Igdcc4 or Prtg.

The carbohydrate chains of glycoproteins are frequently capped by negatively charged sialic acid residues (Varki et al., 2009), and sialylation can interfere with receptor ligand interactions (Quast et al., 2015). When cerebellar extracts were subjected to two dimensional gel electrophoresis (2DGE) and immunoblotted with anti-Cbln1 antiserum, multiple spots of Cbln1-like ir were evident [Fig. 4a]. Five of these spots, of the same molecular weight, but disparate isoelectric points (pI), were deemed specific based upon their absence in extracts from Cbln1-null cerebellum and known enhanced expression in Cbln3-null cerebellum [circles, Fig. 4a] (Bao et al., 2006).

Two of the spots were more acidic than the predicted pI of Cbln1 (pI=5.9). To determine whether the charge heterogeneity of Cbln1 was attributable to sialic acid, HA-Cbln1 was digested with neuraminidase and run on 2DGE IB [Fig. 4b]. Untreated HA-Cbln1 ran as at least 7 spots of the same molecular weight and pI more acidic than the predicted pI of HA-Cbln1 (pI=5.23) [Fig 6b]. Digestion with neuraminidase, but not heat-inactivated neuraminidase resulted in the disappearance of more acidic spots and accumulation of more neutral spots [Fig. 4b], without changing molecular weight [Fig. 4c]. As loss of glycosylation in Cbln1 resulted in gain of Nrxn and Grid2 binding we examined whether neuraminidase treatment conferred gain of receptor binding [Fig. 4d]. No discernible differences in HA-Cbln1 binding to Nrxn1 or Grid2 were evident following desialylation. As Nrxn1 binding is much greater than Grid2 binding, two exposures are shown for clarity [Fig. 4d].

As Cbln4 uniquely binds DCC and monoglycosylated Cbln4 gains Grid2 binding, we examined whether neuraminidase treatment affects these parameters. 2DGE IB of recombinant HA-Cbln4 reveal numerous poorly resolved spots of similar molecular weights [Fig. 5a]. The majority of spots are more acidic than the predicted pI of HA-Cbln4 (pI=5.9). Treatment with neuraminidase eliminates the most acidic spots [Fig. 5a] without affecting

molecular weight [Fig. 5a, b]. However, neuraminidase treatment did not uncover Grid2 binding [Fig. 5b].

Carbohydrate chains on proteins create distinct structural elements that can influence interactions with other molecules (Hanson et al., 2009; Nyathi et al., 2013). Secreted Cblns are homo- and heteromeric complexes composed of six subunits, assembled into a dimer of trimers (Bao et al., 2005). Since monoglycosylated Cblns showed altered binding, we asked whether glycosylation influenced complex composition or stoichiometry. Co-immunoprecipitation (IP) of Myc-tagged monoglycosylated forms of Cbln1 [Fig. 6a] and Cbln4 [Fig. 6b] with HA-tagged WT Cbln1, Cbln2, Cbln3 and Cbln4 showed that all variants formed heteromeric complexes with all other Cbln family members. Co-IP of Myc- and HA-tagged WT and monoglycosylated Cbln1 [Fig. 6c] and Cbln4 [Fig. 6d] revealed that monoglycosylated versions also form complexes with WT or monoglycosylated variants. Thus, glycosylation does not influence Cbln complex composition.

The size of Cbln-containing complexes can be investigated by native gel electrophoresis (Bao et al., 2005). WT Cbln1, Cbln2 or Cbln4-containing complexes behave as hexamers [Fig. 7a upper panel]. Glycosylation mutants also behaved as hexamers with only Cbln4^{N26Q} favoring production of a larger complex [Fig. 7a]. Thus, glycosylation does not markedly affect the formation or composition of hexameric complexes.

Glycosylation site mutants were obtained by mutating asparagine to glutamine and so the possibility exists that this amino acid change alone rather than loss of the glycan results in enhanced binding. To address this concern, we generated unglycosylated or partially glycosylated forms of Cbln4 by inhibition of N-linked glycan synthesis using tunicamycin (Elbein AD, 1987). Tunicamycin showed concentration dependent glycosylation changes on Cbln4, resulting in secretion of mono or unglycosylated forms of the protein (Fig 7b).

Unglycosylated and partially glycosylated Cbln4 from tunicamycin treated cells bound to Nrxn1, Grid2 and DCC to a much greater extent than fully glycosylated Cbln4 (Fig 7b). These data are consistent with the results obtained using asparagine to glutamine mutant Cbln4 (Fig 2) and reinforce our hypothesis that glycans are inhibitory to the binding of Cblns with its receptors.

Targeted expression of Cbln1 or Cbln2 in Purkinje neurons of transgenic mice using the Purkinje cell-specific L7-promoter (Oberdick et al., 1990) prevents cerebellar deficits in Cbln1-null mice (Rong et al., 2012). As glycosylation mutants of Cbln4 bind Grid2 in vitro we hypothesized they would rescue Cbln1 deficiency *in vivo* and tested this using the same L7 promoter-based strategy [Fig. 8a]. We derived transgenic mice expressing L7-Cbln4, L7-Cbln4^{N26Q} or L7-Cbln4^{N85Q} in Purkinje cells. A TaqMan qPCR copy number assay showed that the L7-Cbln4 line had 22 copies, the L7-Cbln4^{N26Q} line had 7 copies and the L7-Cbln4^{N85Q} line had 45 copies of the transgene, respectively [Fig. 8b].

The relative levels of mRNA expression in different transgenic lines was measured by Northern blotting of total cerebellar RNA with an L7 probe that detects endogenous L7 mRNA (internal loading control) and the common component of larger L7-Cbln1, L7-Cbln2, L7-Cbln4, L7-Cbln4^{N26Q} and L7-Cbln4^{N85Q} fusion mRNAs [Fig. 8c]. This permitted

quantitative comparison of mRNA levels in multiple L7-Cbln4 transgenic lines and comparison to levels of mRNA for L7-Cbln1 and L7-Cbln2 in the two strains of transgenic mice that rescue function in Cbln1-null mice (Rong et al., 2012). The mRNA level in L7-Cbln4 was similar to the L7-Cbln1 line, but less than the L7-Cbln2 line [Fig. 8c]. The expression levels of L7-Cbln4^{N26Q} and L7-Cbln4^{N85Q} mRNAs were lower than those of L7-Cbln1, L7-Cbln2 and L7-Cbln4 [Fig. 8c].

To ensure expression of L7-Cbln4 mRNAs reflected Cbln4 protein levels, and that expression was confined to Purkinje cells, Cbln4 immunohistochemistry was performed. Cbln4-like immunoreactivity (ir) was not detectable in cerebellum of non-transgenic mice [Fig. 8d(i, v)]. In contrast, punctate Cbln4-like ir was observed in Purkinje cells, but not other cerebellar neurons, of L7-Cbln4 [Fig. 8d(ii, vi)], L7-Cbln4^{N26Q} [Fig. 8d(iii, vii)] and L7-Cbln4^{N85Q} [Fig. 8d(iv, viii)]. The punctate staining is similar to that in L7-Cbln1 and L7-Cbln2 mice (Rong et al., 2012), suggesting similar modes of metabolism. The intensity of Cbln4-like ir was noticeably higher in the L7-Cbln4 line compared to the monoglycosylation mutants [Fig. 8d(ii, vi)], consistent with the higher L7-Cbln4 mRNA expression [Fig. 8c].

To investigate whether WT Cbln4 or its monoglycosylation mutants rescued ataxia in Cbln1-null mice or themselves caused locomotor dysfunction, we generated Cbln1-null mice carrying one of the L7-Cbln4 [Fig. 9a], L7-Cbln4^{N26Q} [Fig. 9b], or L7-Cbln4^{N85Q} [Fig. 9c] transgenes and measured motor coordination (45–55 days old; n = 6–8 for each genotype). WT mice and WT mice harboring any of the Cbln4 transgenes were indistinguishable on rotarod performance (data not show), implying putative gain of function does not cause a locomotor deficit. The presence of the L7-Cbln4 allele significantly improved Cbln1-null performance ($p<0.01$), although it was still statistically lower than WT performance ($p<0.001$) [Fig. 9a]. The Cbln4 monoglycosylation mutant transgenes significantly increased latency to fall on a Cbln1-null background (L7-Cbln4^{N26Q} $p<0.001$; L7-Cbln4^{N85Q} $p<0.001$) and were statistically indistinguishable from wild type controls [Fig. 9b, 9c]. Despite their lower levels of expression, monoglycosylated forms of Cbln4 improved locomotor performance to a greater extent than WT Cbln4, implying the mutants are more potent.

3. Discussion

The present study establishes that the N-linked carbohydrate chains of Cbln1, 2 and 4 impair receptor binding *in vitro*. This phenomenon is domain and receptor-dependent. Elimination of the N-terminal N-glycan in Cbln1, Cbln2 and Cbln4 enhances Nrxn binding [Fig. 2], which interacts with this region, and has a lesser potentiating effect on Grid2 binding that involves the C1q domain (Elegheert et al., 2016; Cheng et al., 2016). In contrast, Cbln1 and Cbln2 binding to Grid2 is greatly enhanced by elimination of their C1q glycosylation sites with lesser effects on Nrxn binding. In the case of Cbln4, mutation of its C1q glycosylation site enhances its known DCC binding and uncovers potent cryptic Grid2 binding that could explain its ability to rescue Cbln1 loss of function *in vivo*. The attenuation of Cbln binding and activity by glycosylation is reminiscent of the action of glycosylation in TNFα. This cytokine is structurally similar to Cblns, and its glycosylation limits its biological activity (Koyama et al., 1992).

A key question is how glycosylation of the ligand influences its receptor binding. One possibility is that N-glycans alter subunit stoichiometry of the secreted complexes. For example, if reduced glycosylation changed the complex from a hexamer (dimer of trimers) to a dodecamer (tetramer of trimers), thereby potentially doubling the number of receptor binding interfaces, the ligand binding affinity should increase exponentially. As Cbln complexes withstand native gel electrophoresis, this is used to assess their apparent molecular mass (Bao et al., 2005). Compared to WT, glycosylation mutants of Cblns behaved as hexamers, with slightly reduced mass, due to the smaller protomers. Only $Cbln4^{N26Q}$ showed any evidence of higher order complexes. Furthermore, glycosylation did not affect binding interactions amongst different family members. Thus, glycosylation does not affect the number or type of subunits in Cbln complexes.

Sialylation is known to interfere with receptor-ligand interactions. For example, sialic acid reduces the binding of complement C1q, which is structurally very similar to Cbln1, to its IgG Fc receptor and inhibits immediate proinflammatory IgG effector functions (Quast et al., 2015). Unglycosylated recombinant Cbln1 is predicted to have a pI of 5.9. However, on 2DGE Cbln1 resolves into multiple (at least 6) species differing only in their pIs. A similar heterogeneity is observed for native Cbln1 in cerebellar extracts [Fig. 4a]. The predominant reason for heterogeneity is the varying content of sialic acid, as treatment with neuraminidase shifts the pI to higher pH values close to that of unglycosylated Cbln1. Despite the presence of sialic acid on Cbln1 and Cbln4, treatment with neuraminidase did not affect binding to Nrxn or Grid2; suggesting a larger segment of the glycan, if not its entirety is required to impair binding. Therefore, the carbohydrates must either interact with the amino acid backbone of the monomer to influence its 3D structure and thereby receptor binding or the carbohydrates could physically overlie the receptor-binding domain and impair binding via steric hindrance.

Cbln proteins belong to the C1q/TNF superfamily. The 3-D structure of the C-terminal globular domain of human C1q was determined by X-ray crystallography (Gaboriaud et al., 2003) and is a globular, almost spherical heterotrimeric assembly, with the N- and C-termini of each subunit emerging at the base of the trimer. Each subunit exhibits a 10-stranded β sandwich fold with a jelly roll topology homologous to that described initially for tumor necrosis factor (Eck et al., 1989). Comparison of the C1q/TNF superfamily indicates strong conservation of the β-strands but variability in the loops connecting them (Ressl et al., 2015). The recent Cbln1-Grid2 structural analysis shows that the Cbln1 C1q domain binds the Grid2 extracellular amino-terminal domain via loops AA′, CD, EF, and GH from one C1q subunit [Fig. 1a] (Elegheert et al., 2016; Cheng et al., 2016). Cbln1 residues Thr70, Asn71, His72 of loop AA′ and Lys181 of loop GH form a putative hydrogen-bonding network to Grid2 at residue Asp24. The Cbln1 C1q domain N-glycosylation site (Asn79) is located on the αA helix within loop AA′ [Fig. 1a]. The αA helix is a unique structural element of the Cbln family, with no other C1q structures containing these αA helices (Zhong et al., 2017). The C1q domain N-glycan modification could interfere with the ligand-receptor binding interface within loop AA′. Alternatively, or in addition, it might affect the three dimensional configuration of Cblns, potentially by promoting the αA helix, and thereby modifying binding to Grid2. In this scenario distortion of the protomer structure around the Grid2 binding site would reduce ligand affinity. By comparing crystal structures

of the C1q domains of Cbln1 and Cbln4, Zhong et al., (2017) hypothesized that loop CD divergence could account for the inability of Cbln4 to bind with Grid2. The structures of Cbln1 or Cbln4 obtained by Elegheert et al., (2016), Cheng et al., (2016) and Zhong et al., (2017) all used glycosylated proteins to define the Cbln-Grid2 interface. There is no data published to date of the structure of monoglycosylated Cblns and the affect these modifications have on Cbln-Nrxns or Cbln-Grid1/2 complexes. Therefore, our data might prompt an exploration of this subject and may permit precise biophysical measurements of ligand-Grid2 affinities which have been elusive to date due to their weak interactions.

There are increasing examples of extracerebellar synaptic and behavioral functions of Cblns (Kusnoor et al., 2010; Otsuka et al., 2016; Krishnan et al., 2017; Zhang et al., 2017). However, the mechanisms underlying these phenomena are less understood. Therefore, our demonstration that glycosylation mutants of Cblns are more active than their WT counterparts *in vivo* and *in vitro* could be utilized to develop tools to dissect these extracerebellar phenotypes.

4. Experimental procedures

4.1. Animals

WT FVB/NJ and C57BL/6J mice were obtained from Jackson Laboratory (Bar Harbor, ME). All genetically modified strains of mice were generated at St. Jude Children's Research Hospital. Mice were maintained at St. Jude Children's Research Hospital with free access to food and water on a 12:12 h light:dark cycle. Investigational procedures conformed to all applicable federal rules and guidelines and were approved by the St. Jude Children's Research Hospital Animal Care and Use Committee.

4.2. Generation of L7-Cbln transgenic mice

L7-Cbln transgenic mice were generated as described previously (Oberdick et al., 1990; Rong et al., 2012). Mice were genotyped by polymerase chain reaction (PCR) using the primers: L7-Cbln4 (F) 5′-TGA GCC TCA TGT TGA ACG GG-3′, L7-Cbln4 (R) 5′-ATG ATG ATC CCT TGG AGT-3′. Relative expression of transgenes was determined by northern blotting (Rong et al., 2012). Strains with the highest expression were mated with $Cbln1^{+/-}$ mice to generate appropriate genotypes for analysis.

4.3. Transgene copy number measurement

Genomic DNA was isolated using the DNeasy Tissue kit (Qiagen, Valencia, CA) and L7 transgene copy number determined by quantitative real-time PCR (qPCR). Mouse-specific TaqMan Copy Number Assays for Pcp2 (L7) and Cbln3 (known copy number control) were purchased from Thermo Fisher Scientific (Waltham, MA, Pcp2, Mm00260051_cn; Cbln3, Mm00605149_cn). qPCR was performed using 2x TaqMan Fast Reagents Starter Kit and the ABI 7900 Fast Real-Time PCR system (Thermo Fisher Scientific). PCR conditions were: uracil-N-glycosylase incubation, 50°C for 2 min, AmpliTaq Gold activation, 95°C for 10 min, denaturation 95°C for 15 s, annealing 60°C for 1 min (40 cycles).

4.4. Plasmids and constructs

Full-length murine N-terminal hemagglutinin (HA)-tagged Cbln1, Cbln2, Cbln3, and Cbln4 (Rong et al., 2012; Wei et al., 2012) were sub-cloned into pcDNA3.1 vector (Thermo Fisher Scientific) as the backbones for mutagenesis. Myc-tagged Cbln1 and Cbln4 were generated similarly. Full-length FLAG-tagged murine Grid1, Grid2, Nrxn1β, Nrxn1β S4^{-}, Nrxn3β, Nrxn3β S4^{-}, neogenin 1 (Neo1), Igdcc3, Igdcc4, Prtg and human DCC were sub-cloned into p3XFLAG-CMV™-14 Expression Vector (Sigma-Aldrich, St. Louis, MO) (Wei et al., 2012). Mutations were generated using the QuikChange II XL site-directed mutagenesis kit (Agilent Technologies, Santa Clara, CA).

4.5. Deglycosylation

Conditioned medium containing WT or glycosylation mutants of HA-Cbln1, HA-Cbln2 or HA-Cbln4 (50 μl) were digested with PNGase F (New England Biolabs, Ipswich, MA) as described previously (Hirai et al., 2005).

4.6. In vitro binding assay

The binding of WT and glycosylation mutants of Cblns to Grid1, Grid2, Nrxn1β, Nrxn1βS4^{-}, Nrxn3β, Nrxn3βS4^{-}, DCC, Neo1, Igdcc3, Igdcc4 and Prtg was studied using published methods (Rong et al., 2012; Wei et al., 2012). Briefly, medium containing the HA-tagged ligands was collected 48 h after transfection and transferred to cells expressing FLAG-tagged receptor. After 4 h, cells were washed three times with ice-cold medium, lysed with 1x XT sample buffer (Bio-Rad, Hercules, CA) containing 10 mM Dithiothreitol (DTT), electrophoresed on Criterion 4–12% Bis-Tris gels (Bio-Rad), transferred to nitrocellulose membranes and incubated with anti-HA (BioLegend, San Diego, CA) or anti-Cbln1 (Bao et al., 2005) antibodies to detect ligands and anti-FLAG mouse monoclonal antibody (Sigma-Aldrich) to detect receptors. The blots were incubated with Horseradish Peroxidase-conjugated secondary antibodies (GE Healthcare, Chicago, IL) and immunoreactive bands were detected using a chemiluminescence system (Thermo Fisher Scientific). Signals were captured using an Odyssey Fc Imaging System (LI-COR Biosciences, Lincoln, NE). Band intensities were quantified using Image Studio (LI-COR Biosciences). For quantification, band intensities for 3 separate experiments were corrected for input and analyzed by Student's *t*-test.

4.7. Two dimensional gel electrophoresis (2DGE)

Cerebellar P2 fractions (Gray and Whittaker 1962) or conditioned medium from HEK293T cells (PRID: CRL-3216) (ATCC, Manassas, VA) expressing Cblns were precipitated with TCA. Pellets were suspended in 200 μl of rehydration buffer (Bio-Rad). Isoelectric focusing was performed on 11 cm immobilized pH 4–7 or pH 5–8 gradient ReadyStrip IPG strips (Bio-Rad). Second dimensional gel electrophoresis was performed using Bio-Rad's 4–12% Criterion XT Bis-Tris precast polyacrylamide gels. Proteins were transferred to nitrocellulose membranes (0.2 microns) using iBlot semi-dry transfer conditions (Thermo Fisher Scientific), and IB performed using anti-HA antibodies (RRID: AB_2565335) or rabbit antibodies against Cbln1 (Bao et al., 2005).

4.8. Desialylation

Conditioned medium from HEK293T cells expressing HA tagged proteins was incubated with GlycoCleave neuraminidase absorbent beads (GALAB Technologies GmbH, Germany), heat-inactivated beads (95°C 10 min) or no beads at 37°C for 3 h or 18 h for Cbln1 and 6 h for Cbln4. 2DGE IB was also performed on Cbln1 and Cbln4 samples to confirm removal of sialic acid.

4.9. Co-immunoprecipitation (IP)

Conditioned medium from HEK293T cells expressing combinations of Myc and HA epitope containing proteins was collected after 48 h of transfection and was spun down at 5000 rpm for 5 min to remove any cells or cell debris. Medium was concentrated 4 times using 3000 MWCO spin filter (Millipore) and a final concentration of 1x was obtained by diluting with IP buffer containing 50 mM Tris-HCl pH 7.4, 120 mM NaCl, 0.5% NP-40, 0.25% sodium deoxycholate along with EDTA-free protease inhibitor cocktail (Roche, Mannheim, Germany). After pre clearing with Protein A Sepharose CL-4B (GE Healthcare), 2.5 μg of mouse anti-HA antibody (Biolegend) was added and samples were incubated over night at 4 °C. Subsequently, 20 μl of buffer-washed Protein A Sepharose CL-4B was added and incubation was continued for another 1 h at 4 °C. Beads were washed three times with IP buffer and suspended in 50 μl of 1x XT sample buffer containing 50 mM DTT solution. Immunoprecipitated samples were analyzed by separating on sodium dodecyl sulfate polyacrylamide gel electrophoresis (SDS-PAGE) and immunoblotting the membranes with rabbit anti-HA (Cell Signaling, Danvers, MA) and rabbit anti-Myc (Merck Millipore, Burlington, MA) antibodies.

4.10. Native gel electrophoresis

Conditioned medium from HEK293T cells expressing HA-tagged WT or mutant Cblns was mixed with an equal volume of native sample buffer (Bio-Rad). Samples were separated on precast 7.5% Tris-HCl Criterion gels (Bio-Rad), transferred onto nitrocellulose membranes, immunoblotted using anti-HA antibody and signal visualized by chemiluminescence (Thermo Fisher Scientific). Native protein standards (Thermo Fisher Scientific) were run on independent gels and stained with SYPRO Ruby Protein Gel Stain (Sigma-Aldrich) and visualized by ultra violet light using a Gel Doc system (Alpha Innotech, San Leandro, CA).

4.11. Tunicamycin assay

HEK293T cells were transfected with vectors carrying HA epitope tagged Cbln4 in six well plates. After 4 hours of transfection, HEK293T cells were exposed to different concentrations of tunicamycin (Sigma-Aldrich) for 42 hours. Conditioned media containing secreted proteins was collected and centrifuged at 2000 rpm for 5 min to remove any cell debris. Clear supernatant containing secreted HA-Cbln4 was added to HEK293T cells expressing one of FLAG-tagged Nrxn1, DCC or Grid2 in a binding assay as described in section 4.6 above.

4.12. Histologic methods

Three-month-old mice were anesthetized and perfused transcardially with buffered 4% paraformaldehyde and the brains were removed and processed for paraffin-embedding as described previously (Wei et al., 2007). 5-μm sagittal sections were stained with hematoxylin and eosin for standard histological analysis. For immunohistochemistry, sections were subjected to heat-mediated antigen retrieval in 0.01 M sodium citrate buffer (pH 6.0) containing 0.05% Tween 20 (Sigma-Aldrich) as described (Wei et al., 2009). Immunostaining for Cbln4 was performed using rabbit anti-Cbln4 (1:300, Aviva Systems Biology, San Diego, CA). Immunocomplexes were revealed using a peroxidase-conjugated anti-rabbit antiserum and diaminobenzidine tetrahydrochloride (DAB) substrate (Dako, Carpenteria, CA).

4.13. Rotarod test

Mice were randomly assigned to different cages (1–5/cage) when they were 21-days old. The mice (20–30 g/mouse; 45–50 days old; 6–8 mice/group) were tested on an accelerating rotarod (San Diego Instruments, San Diego, CA) to assess motor coordination, balance, and motor learning (Buitrago et al., 2004; Wei et al., 2011; Rong et al., 2012). The rotarod accelerated from 0 to 40 rpm in 4 min and then maintained constant speed for 1 min. The time elapsed before the mouse fell (latency to fall) was recorded. The maximum observation time was 5 min. Animals received 2 trials per day, with a 20-min inter-trial interval for 5 consecutive days (Monday–Friday; 9AM–11AM, the order in which animals were tested was randomized). Data include all tested animals, and were expressed as mean ± SEM and analyzed for statistical significance using repeated-measures analysis of variance (ANOVA). Where appropriate multiple-comparison tests were performed with Bonferroni's adjustment. The level of significance was set at $p < 0.05$.

4.14. Statistical analysis

Student's t-test was used unless otherwise stated. Significance was set at a p of < 0.05. All statistical analyses were performed using SAS version 9.2 (SAS Institute Inc., Cary, NC).

Acknowledgments

This work was supported in part by ALSAC (American Lebanese Syrian Associated Charities) and Cancer Center Support Grant (P30 CA021765) to J. I. Morgan.

Abbreviations

2DGE	two dimensional gel electrophoresis
ANOVA	one-way analysis of variance
Cbln	cerebellin precursor protein
DCC	deleted in colorectal carcinoma
DTT	Dithiothreitol
Grid	glutamate receptor, ionotropic, delta

HA	hemagglutinin
IB	immunoblotting
IP	immunoprecipitation
ir	immunoreactivity
KO	knockout
Nrxn	neurexin
pI	isoelectric points
qPCR	quantitative PCR
PCR	polymerase chain reaction
SDS-PAGE	sodium dodecyl sulfate polyacrylamide gel electrophoresis
WT	wild type

References

Bao D, Pang Z, Morgan JI. The structure and proteolytic processing of Cbln1 complexes. J Neurochem. 2005; 95:618–629. [PubMed: 16135095]

Bao D, Pang Z, Morgan MA, Parris J, Rong Y, Li L, Morgan JI. Cbln1 is essential for interaction-dependent secretion of Cbln3. Mol Cell Biol. 2006; 26:9327–37. [PubMed: 17030622]

Buitrago MM, Schulz JB, Dichgans J, Luft AR. Short and long-term motor skill learning in an accelerated rotarod training paradigm. Neurobiol Learn Mem. 81:211–216.

Castets M, Broutier L, Molin Y, Brevet M, Chazot G, Gadot N, Paquet A, Mazelin L, Jarrosson-Wuilleme L, Scoazec JY, Bernet A, Mehlen P. DCC constrains tumor progression via its dependence receptor activity. Nature. 2012; 482:534–537.

Cheng S, Seven AB, Wang J, Skiniotis G, Özkan E. Conformational Plasticity in the Transsynaptic Neurexin-Cerebellin-Glutamate Receptor Adhesion Complex. Structure. 2016; 24:2163–2173. [PubMed: 27926833]

Eck MJ, Sprang SR. The structure of tumor necrosis factor-alpha at 2.6 A resolution. Implications for receptor binding. J Biol Chem. 1989; 264:17595–17605. [PubMed: 2551905]

Elbein AD. Inhibitors of the biosynthesis and processing of N-linked oligosaccharide chains. Annu Rev Biochem. 1987; 56:497–534. [PubMed: 3304143]

Elegheert J, Kakegawa W, Clay JE, Shanks NF, Behiels E, Matsuda K, Kohda K, Miura E, Rossmann M, Mitakidis N, Motohashi J, Chang VT, Siebold C, Greger IH, Nakagawa T, Yuzaki M, Aricescu AR. Structural basis for integration of GluD receptors within synaptic organizer complexes. Science. 2016; 353:295–299. [PubMed: 27418511]

Gaboriaud C, Juanhuix J, Gruez A, Lacroix M, Darnault C, Pignol D, Verger D, Fontecilla-Camps JC, Arlaud GJ. The crystal structure of the globular head of complement protein C1q provides a basis for its versatile recognition properties. J Biol Chem. 2003; 278:46974–46982. [PubMed: 12960167]

Gray EG, Whittaker VP. The isolation of nerve endings from brain: An electron microscopic study of cell fragments derived by homogenization and centrifugation. J of Anatomy. 1962; 96:79–88.

Haddick PC, Tom I, Luis E, Quiñones G, Wranik BJ, Ramani SR, Stephan JP, Tessier-Lavigne M, Gonzalez LC. Defining the ligand specificity of the deleted in colorectal cancer (DCC) receptor. PloS one. 2014; 9:e84823. [PubMed: 24400119]

Han L, Zhang D, Tao T, Sun X, Liu X, Zhu G, Xu Z, Zhu L, Zhang Y, Liu W, Ke K, Shen A. The role of N-glycan modification of TNFR1 in inflammatory microglia activation. Glycoconj J. 2015; 32:685–93. [PubMed: 26452604]

Hanson SR, Culyba EK, Hsu TL, Wong CH, Kelly JW, Powers ET. The core trisaccharide of an N-linked glycoprotein intrinsically accelerates folding and enhances stability. Proc Natl Acad Sci USA. 2009; 106:3131–3136. [PubMed: 19204290]

Hirai H, Pang Z, Bao D, Miyazaki T, Li L, Miura E, Parris J, Rong Y, Watanabe M, Yuzaki M, Morgan JI. Cbln1 is essential for synaptic integrity and plasticity in the cerebellum. Nat Neurosci. 2005; 8:1534–41. [PubMed: 16234806]

Jiang Y, Liu MT, Gershon MD. Netrins and DCC in the guidance of migrating neural crest-derived cells in the developing bowel and pancreas. Dev Boil. 2003; 258:364–384.

Joo JY, Lee SJ, Uemura T, Yoshida T, Yasumura M, Watanabe M, Mishina M. Differential interactions of cerebellin precursor protein (Cbln) subtypes and neurexin variants for synapse formation of cortical neurons. Biochem Biophys Res Commun. 2011; 406:627–632. [PubMed: 21356198]

Koyama Y, Hayashi T, Fujii N, Yoshida T. Recombinant mouse tumor necrosis factor expressed in mammalian cells: effect of glycosylation on cytotoxic activity. Biochim Biophys Acta. 1992; 1132:188–194. [PubMed: 1390889]

Krishnan V, Stoppel DC, Nong Y, Johnson MA, Nadler MJS, Cruz J, Kasper EM, Arnaout R, Anderson MP. Autism gene Ube3a and seizures impair sociability by repressing VTA Cbln1. Nature. 2017; 543:507–512. [PubMed: 28297715]

Kusnoor SV, Parris J, Muly EC, Morgan JI, Deutch AY. Extracerebellar role for Cerebellin1: modulation of dendritic spine density and synapses in striatal medium spiny neurons. J Comp Neurol. 2010; 518:2525–2537. [PubMed: 20503425]

Matsuda K, Miura E, Miyazaki T, Kakegawa W, Emi K, Narumi S, Fukazawa Y, Ito-Ishida A, Kondo T, Shigemoto R, Watanabe M, Yuzaki M. Cbln1 is a ligand for an orphan glutamate receptor delta2, a bidirectional synapse organizer. Science. 2010; 328:363–368. [PubMed: 20395510]

Mehlen P, Rabizadeh S, Snipas SJ, Assa-Munt N, Salvesen GS, Bredesen DE. The DCC gene product induces apoptosis by a mechanism requiring receptor proteolysis. Nature. 1998; 395:801–804. [PubMed: 9796814]

Mehlen P, Rama N. Netrin-1 and axonal guidance: signaling and asymmetrical translation. Med Sci (Paris). 2007; 23:311–315. [PubMed: 17349294]

Nyathi Y, Wilkinson BM, Pool MR. Co-translational targeting and translocation of proteins to the endoplasmic reticulum. Biochim Biophys Acta. 2013; 1833:2392–2402. [PubMed: 23481039]

Oberdick J, Smeyne RJ, Mann JR, Zackson S, Morgan JI. A promoter that drives transgene expression in cerebellar Purkinje and retinal bipolar neurons. Science. 1990; 248:223–226. [PubMed: 2109351]

Otsuka S, Konno K, Abe M, Motohashi J, Kohda K, Sakimura K, Watanabe M, Yuzaki M. Roles of Cbln1 in Non-Motor Functions of Mice. J Neurosci. 2016; 36:11801–11816. [PubMed: 27852787]

Quast I, Keller CW, Maurer MA, Giddens JP, Tackenberg B, Wang LX, Münz C, Nimmerjahn F, Dalakas MC, Lünemann JD. Sialylation of IgG Fc domain impairs complement-dependent cytotoxicity. J Clin Invest. 2015; 125:4160–4170. [PubMed: 26436649]

Ressl S, Vu BK, Vivona S, Martinelli DC, Südhof TC, Brunger AT. Structures of C1q-like proteins reveal unique features among the C1q/TNF superfamily. Structure. 2015; 23:688–699. [PubMed: 25752542]

Ritchie GE, Moffatt BE, Sim RB, Morgan BP, Dwek RA, Rudd PM. Glycosylation and the complement system. Chem Rev. 2002; 102:305–320. [PubMed: 11841245]

Rong Y, Wei P, Parris J, Guo H, Pattarini R, Correia K, Li L, Kusnoor SV, Deutch AY, Morgan JI. Comparison of Cbln1 and Cbln2 Functions using Transgenic and Knockout Mice. J Neurochem. 2012; 120:528–540. [PubMed: 22117778]

Uemura T, Lee SJ, Yasumura M, Takeuchi T, Yoshida T, Ra M, Taguchi R, Sakimura K, Mishina M. Trans-synaptic interaction of GluRdelta2 and Neurexin through Cbln1 mediates synapse formation in the cerebellum. Cell. 2010; 141:1068–79. [PubMed: 20537373]

Urade Y, Oberdick J, Molinar-Rode R, Morgan JI. Precerebellin is a cerebellum-specific protein with similarity to the globular domain of complement C1q B chain. Proc Natl Acad Sci USA. 1991; 88:1069–73. [PubMed: 1704129]

Varki, A., Schauer, R. Essentials of Glycobiology. 2. Varki, A.Cummings, RD.Esko, JD.Freeze, HH.Stanley, P.Bertozzi, CR.Hart, GW., Etzler, ME., editors. Vol. Chapter 14. Cold Spring Harbor (NY): Cold Spring Harbor Laboratory Press; 2009.

Wei P, Smeyne RJ, Bao D, Parris J, Morgan JI. Mapping of Cbln1-like immunoreactivity in adult and developing mouse brain and its localization to the endolysosomal compartment of neurons. Eur J Neurosci. 2007; 26:2962–2978. [PubMed: 18001291]

Wei P, Rong Y, Li L, Bao D, Morgan JI. Characterization of trans-neuronal trafficking of Cbln1. Mol Cell Neurosci. 2009; 41:258–73. [PubMed: 19344768]

Wei P, Blundon JA, Rong Y, Zakharenko SS, Morgan JI. Impaired locomotor learning and altered cerebellar synaptic plasticity in pep-19/PCP4-null mice. Mol Cell Biol. 2011; 31:2838–2844. [PubMed: 21576365]

Wei P, Pattarini R, Rong Y, Guo H, Bansal PK, Kusnoor SV, Deutch AY, Parris J, Morgan JI. The Cbln Family of Proteins Interact with Multiple Signaling Pathways. J Neurochem. 2012; 121:717–729. [PubMed: 22220752]

Zhang B, Seigneur E, Wei P, Gokce O, Morgan JI, Südhof TC. Developmental plasticity shapes synaptic phenotypes of autism-associated neuroligin-3 mutations in the calyx of Held. Mol Psychiatry. 2017; 22:1483–1491. [PubMed: 27725662]

Zhong C, Shen J, Zhang H, Li G, Shen S, Wang F, Hu K, Cao L, He Y, Ding J. Cbln1 and Cbln4 Are Structurally Similar but Differ in GluD2 Binding Interactions. Cell Rep. 2017; 20:2328–2340. [PubMed: 28877468]

Highlights

Glycosylation of Cblns attenuates their receptor binding

Cbln1, 2 and 4 are N-linked glycoproteins. Cbln1 and 2 are ligands that bridge presynaptic neurexins to post-synaptic Grid 2. Cbln4 binds to DCC and has undetectable Grid2 binding *in vitro*. By mutagenesis, we show that glycosylation attenuates Cblns-receptor binding in vitro and appear to gain function in vivo. These findings have implications for the investigation of the burgeoning extracerebellar functions of Cblns and for structural and biophysical studies of Cbln-receptor interactions.

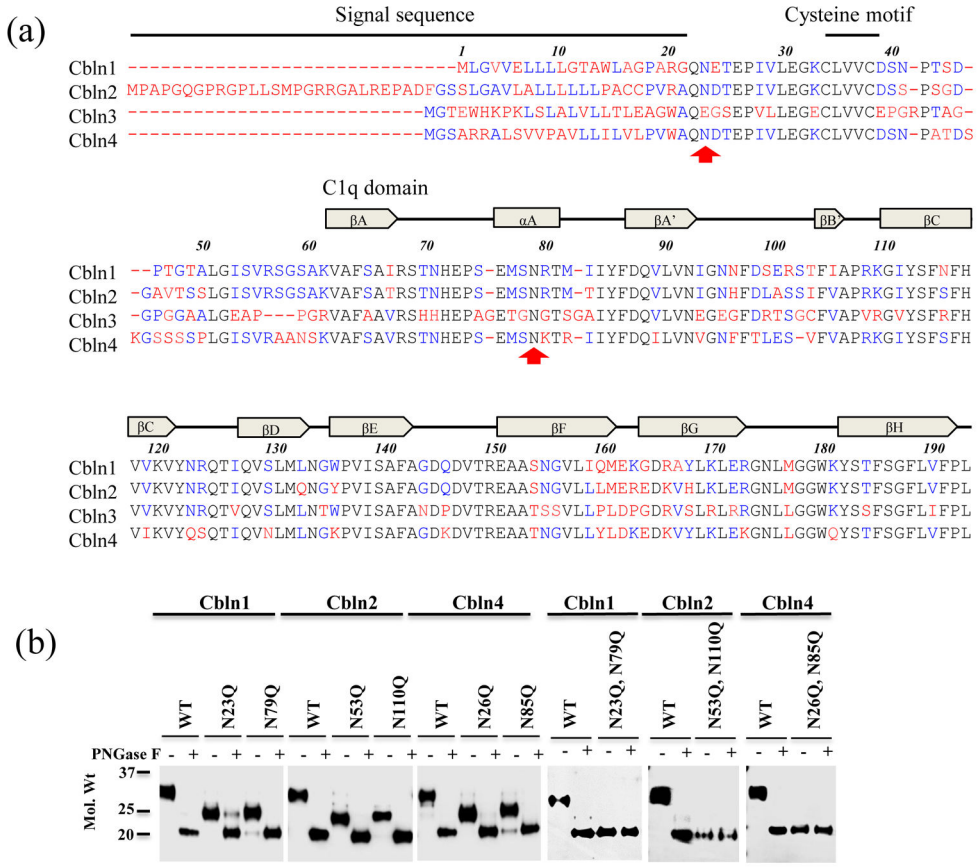

Figure 1.

The Cblns are a family of glycoproteins. (a) Mouse Cbln1–4, amino acid sequences are taken from the NCBI Protein database: Cbln1 (NP_062600), Cbln2 (NP_001289285), Cbln3 (NP_062794), Cbln4 (NP_783439) and aligned using Vector NTI (Thermo Fisher Scientific) to show similarities and differences in amino acid sequences by color coding. The locations of N-linked glycosylation sites are indicated by red arrows. Note Cbln3 lacks an N-terminal glycosylation site. The secondary structure of the Cblns is according to Elegheert et al., (2016). (b) Monoglycosylated and unglycosylated Cblns are secreted proteins. HEK293T cells were transfected with constructs of HA-tagged Cbln1, Cbln2, Cbln4 or their respective asparagine (N) to glutamine (Q) mutants. Secreted proteins were treated with PNGase F and their size determined on SDS-PAGE and IB. (−) buffer only, (+) buffer and PNGase F. Representative results of two independent experiments are shown.

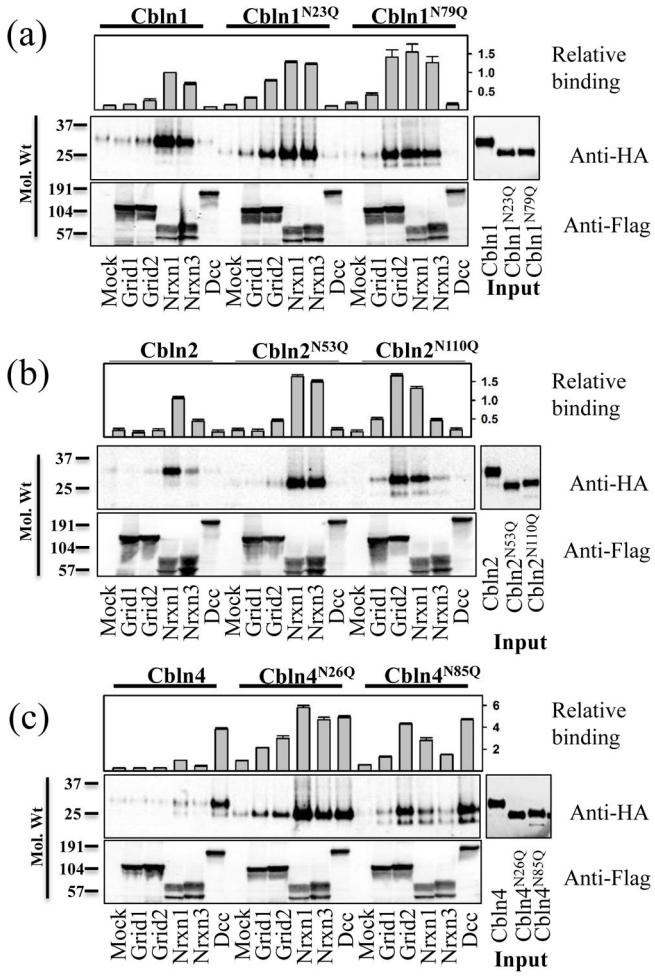

Figure 2.

Comparison of binding of WT and monoglycosylated Cblns to receptors. HEK293T cells were transfected with FLAG-tagged Grid1, Grid2, Nrxn1β, Nrxn3β, DCC or empty vector (mock). Cells were subsequently exposed to conditioned medium (Input) containing HA-tagged Cbln1, Cbln1^{N23Q}, Cbln1^{N79Q}; Cbln2, Cbln2^{N53Q}, Cbln2^{N110Q} and Cbln4, Cbln4^{N26Q}, Cbln4^{N85Q} for 4 h. After washing, cells were lysed, subjected to SDS-PAGE and immunoblotted with anti-HA and anti-FLAG antisera. Quantification was performed on three independent binding assays. (a) Cbln1 bound to Grid2, Nrxn1β, and Nrxn3β, but not to DCC. Cbln1^{N23Q} and notably Cbln1^{N79Q} had greater Grid1 (p<0.05) and Grid2 (p<0.001) binding activity than WT Cbln1. When corrected for input, both glycosylation mutants, and notably Cbln1^{N23Q}, exhibited increased Nrxn binding (Nrxn1β, P<0.01; Nrxn3β, P<0.01). Neither WT Cbln1 nor monoglycosylation mutants bound DCC. (b) Cbln2 bound to Nrxn1β, and Nrxn3β, but had weak or no binding to Grid1, Grid2 or DCC. Cbln2^{N53Q} showed elevated Nrxn1β (P<0.01) and Nrxn3β (P<0.001) binding, and had detectable Grid2 binding (P<0.05). Cbln2^{N110Q} had very high Grid2 binding (P<0.001) and detectable Grid1 binding. Both glycosylation mutants exhibited enhanced Nrxn1β and Nrxn3β binding with the Cbln2^{N53Q} being the more prominent (Nrxn1β, p<0.0001; Nrxn3β, p<0.00001). None of the constructs bound DCC. (c) Cbln4 bound weakly to Nrxn1β and strongly to DCC but did

not bind Grid1 or Grid2. The binding of Cbln4^{N26Q} to Nrxn1β (P<0.001) and Nrxn3β (P<0.001) is greatly increased compared to WT Cbln4. This mutant also bound with Grid1 and Grid2, and DCC binding also increased (p<0.01). Compared to WT Cbln4, Cbln4^{N85Q} showed a increase in binding to Nrxn1β (P<0.01) and Nrxn3β (P<0.001), but showed a massive increase in Grid2 binding (P<0.001). The bar graphs (mean;+/−SD) shown are results of three independent experiments.

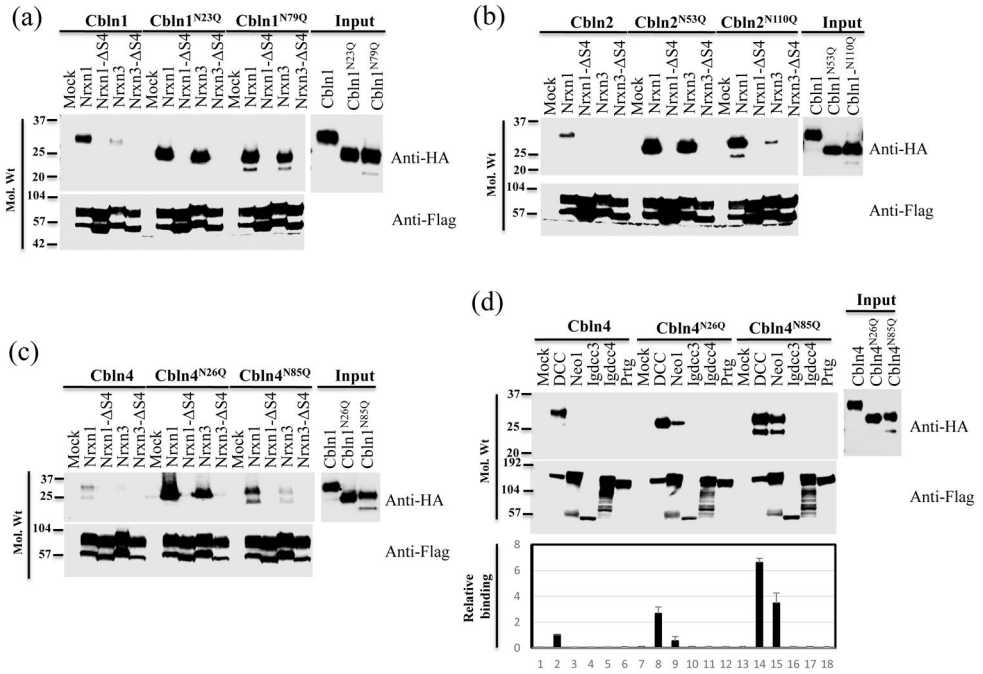

Figure 3.

Monoglycosylated forms of Cblns retain their binding specificity to S4 domains of Nrxns. Conditioned medium from HEK293T cells expressing HA-tagged Cblns were used in a binding assay on HEK293T cells expressing vector (Mock), or FLAG-tagged versions of Nrxns that contained (Nrxn) or lacked (Nrxn-ΔS4) the S4 domain thought to be necessary for Cbln binding. (a) Cbln1 or mutant, (b) Cbln2 or mutant, (c) Cbln4 or mutant. Glycosylation status did not influence Nrxn binding specificity for any of the Cblns. (d) Interaction of Cbln4 monoglycosylated mutants with DCC family members. HA-tagged WT Cbln4 or mutants, were used in binding assays on cells expressing FLAG-tagged DCC, neogenin (Neo1), Igdcc3, Igdcc4 and Prtg. Input: comparative expression levels of proteins used in binding assay. Cbln4^{N26Q} and Cbln^{N85Q} binding with neogenin increased significantly (p=0.045; p=0.017, respectively). Cbln4^{N85Q} binding with DCC also increased (p=0.02). The bar graphs (mean;+/−SD) shown are results of three independent experiments. Representative results of three independent experiments are shown.

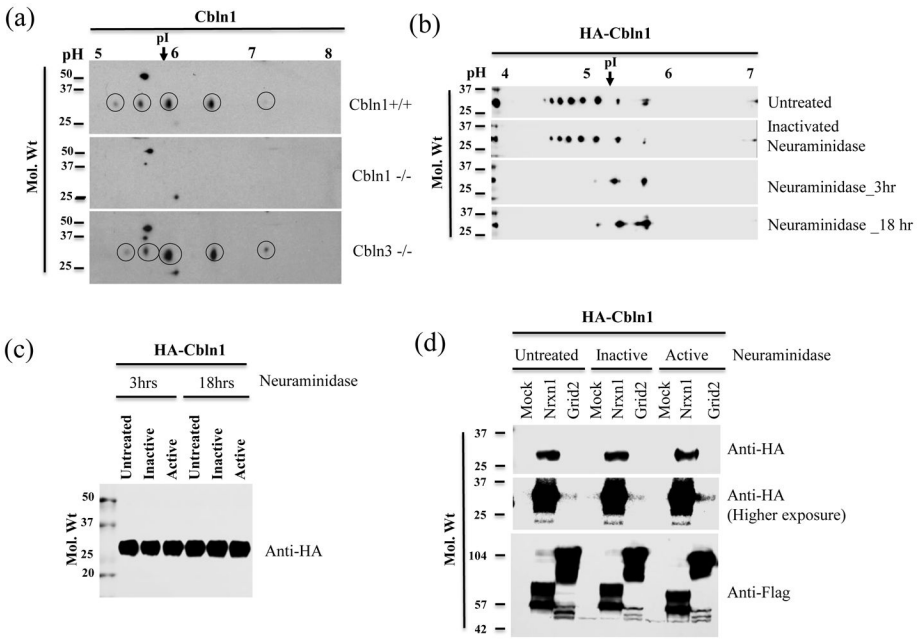

Figure 4.

Cbln1 is a sialoglycoprotein. (a) IB with anti-Cbln1 antibody on 2DGE of Cbln1 in P2 extracts from mouse cerebellum. Based on their absence in Cbln1$^{-/-}$ cerebellum, multiple specific spots are evident (top panel, circled). The intensity of specific spots is increased in extracts from cbln3$^{-/-}$ mice (bottom panel, circled). Specific spots were acidic compared to the theoretical pI of Cbln1 (5.9, arrow in figure). (b) 2DGE of recombinant HA-Cbln1 proteins with or without neuraminidase treatment. Recombinant Cbln1 exhibited multiple spots that were mostly more acidic than the calculated pI (5.23, arrow in figure). Neuraminidase digestion reduced the intensity of acidic spots and increased accumulation of more basic spots. (c) Neuraminidase does not affect the molecular weight of HA-Cbln1. Untreated HA-Cbln1 or HA-Cbln1 treated with heat-inactivated neuraminidase beads or active neuraminidase beads for 3 h or 18 h were separated on SDS-PAGE. (d) Desialylation of Cbln1 does not alter its binding. HEK293T cells expressing vector (Mock), Nrxn1-FLAG or Grid2-FLAG were incubated with neuraminidase treated or untreated HA-Cbln1 conditioned medium for 4 h. Proteins were detected using anti-HA or anti-FLAG antibodies. (Untreated) - conditioned medium alone; (Inactive) - conditioned medium treated with heat inactivated neuraminidase; (Active) - conditioned medium treated with neuraminidase. No statistically significant differences between treated and untreated samples were observed. Neuraminidase treatment and binding assays were performed at least three times.

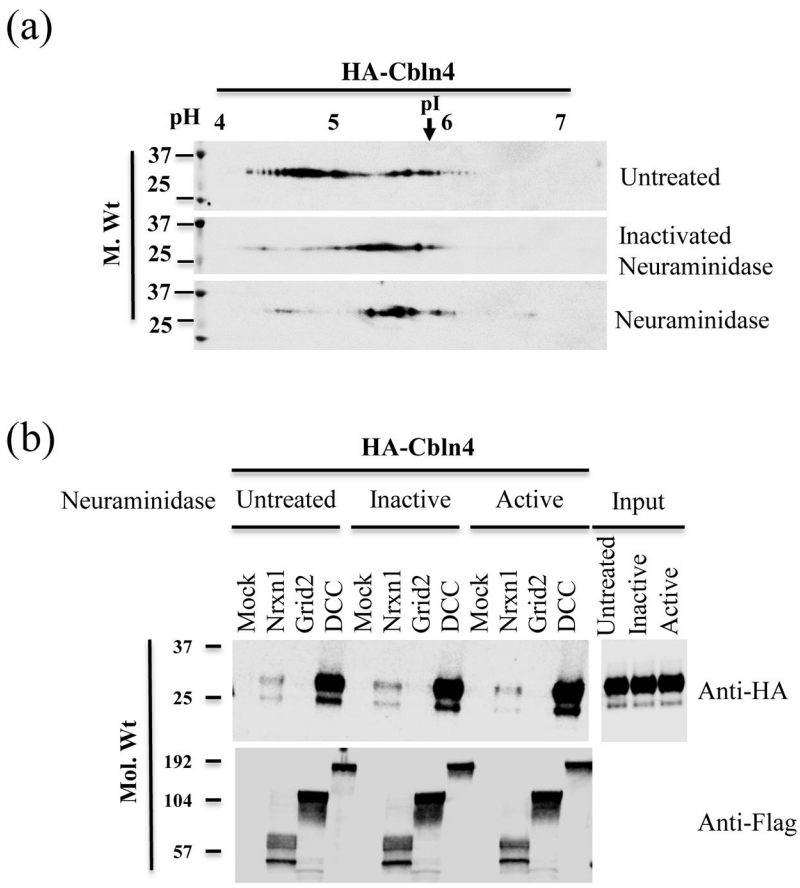

Figure 5.

Cbln4 is also a sialoglycoprotein. (a) Conditioned medium from HEK293T cells containing HA-Cbln4 was subjected to neuraminidase beads treatment for 6 h. Heat inactivated neuraminidase and untreated samples served as controls. Mobility of the treated and untreated proteins was compared on SDS-PAGE after isoelectric focusing. Multiple spots of Cbln4 –ir were detected, the majority being more acidic than the predicted pI of HA-Cbln4 (5.9, arrow in figure) and shifted to more alkaline pI value following neuraminidase digestion. (b) Desialylation does not alter Cbln4 binding. Desialylated Cbln4 (Active) along with heat-inactivated neuraminidase (Inactive) and untreated Cbln4 (Untreated) were used in a comparative binding assay on cells expressing, vector (Mock), Nrxn1-FLAG (Nrxn1), Grid2-FLAG (Grid2) or DCC-FLAG (DCC). No statistically significant differences between treated and untreated samples were observed. Neuraminidase treatment and binding assays were performed at least three times.

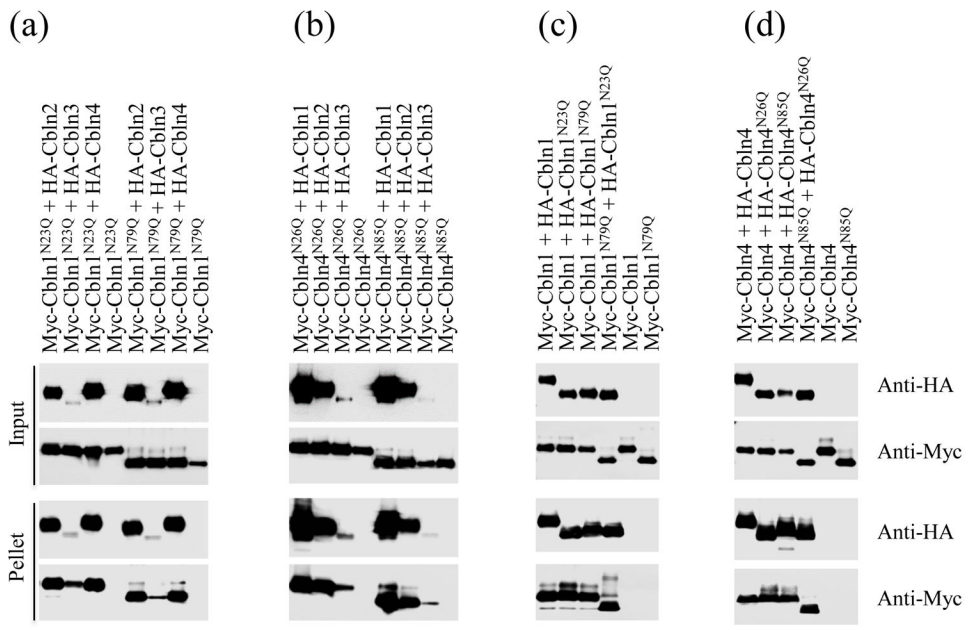

Figure 6.

Glycosylation mutants of Cbln1 and Cbln4 still form homomeric and heteromeric complexes. Conditioned medium from HEK293T cells expressing a single Cbln protein with a Myc epitope or alternatively two different Cbln proteins with Myc and HA epitopes were subjected to co-IP with mouse anti-HA antibody and immunoblotted with rabbit anti-HA or Myc epitope antibodies. (a) HA-tagged Cbln2, Cbln3 or Cbln4 were all able to co-IP with glycosylation mutants of Myc-Cbln1. (b) HA-tagged Cbln1, Cbln2 and Cbln3 were all able to co-IP with glycosylation mutants of Cbln4. (c) HA-Cbln1 or its glycosylation mutants were all able to co-IP Myc-Cbln1 or its glycosylation mutants. (d) HA-Cbln4 or its glycosylation mutants were all able to co-IP with Myc-Cbln4 or its glycosylation mutants.

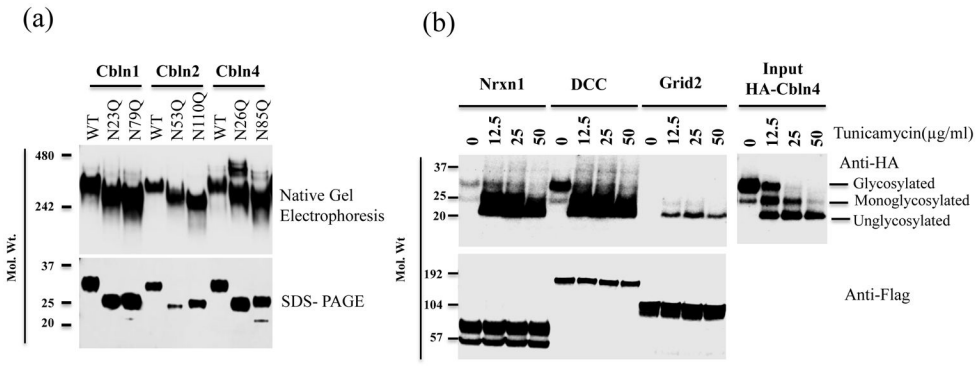

Figure 7.

(a) Monoglycosylated Cblns can form homo-hexameric complexes. Conditioned medium from HEK293T cells expressing HA-tagged Cbln1, Cbln1^{N23Q}, Cbln^{N79Q}, Cbln2, Cbln2^{N53Q}, Cbln2^{N110Q}, Cbln4, Cbln4^{N26Q} and Cbln4^{N85Q} were separated by native gel electrophoresis on 7.5% Tris-HCl gel (upper panel) or by SDS-PAGE (lower panel). Proteins were detected by IB with anti-HA antibody. Molecular weight markers are shown at left. With the exception of Cbln4^{N26Q}, all species behave as hexamers. (b)Wild type Cbln4 functions like monoglycosylation mutants when N-glycan synthesis is inhibited. Conditioned medium from HEK293T cells expressing HA-tagged Cbln4 in the presence of the indicated concentration of tunicamycin (N-glycan chain synthesis inhibitor), was used in a binding assay on cells expressing FLAG-tagged Nrxn1, DCC or Grid2. Inhibition of N-glycan chain synthesis resulted in appearance of monoglycosylated and unglycosylated Cbln4 that bound more avidly to Nrxn1, DCC and Grid2. Input: comparative expression and glycosylation levels of Cbln4 after tunicamycin treatment used in the binding assay. Representative results of three independent experiments are shown.

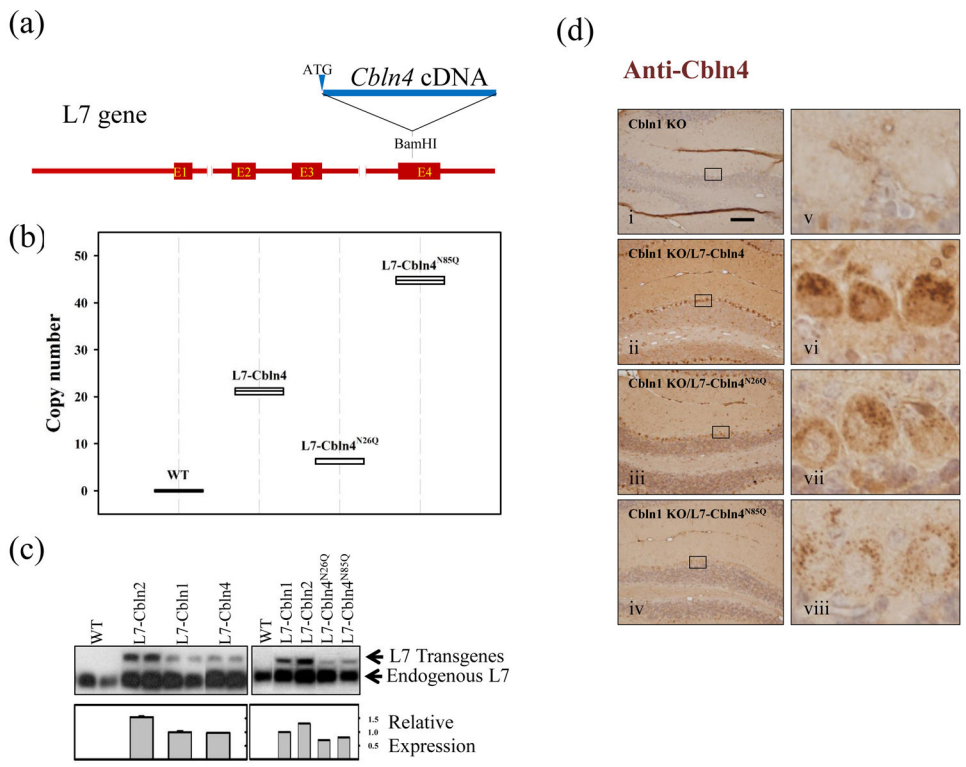

Figure 8.

Ectopic expression of Cbln4, Cbln4^{N26Q} and Cbln4^{N85Q} in Purkinje cells of Cbln1-null mice. (a) WT or monoglycosylation mutant Cbln4 cDNA was inserted into a unique BamHI site in the fourth exon of the L7 gene to make the L7-Cbln4 construct used to generate transgenic mice. (b) TaqMan qPCR amplifications were used to assess copy number of WT Cbln4 or glycosylation mutant lines. Amplifications of transgene (Cbln4) were performed with mouse tail DNA. L7-Cbln4 has 22 copies, L7-Cbln4^{N26Q} had 7 copies and L7-Cbln4^{N85Q} had 45 copies of the transgene (n=4). (d) Northern blot using a probe to L7 on total RNA from the cerebellum of WT, L7-Cbln1, L7-Cbln2, L7-Cbln4, L7-Cbln4^{N26Q} and L7-Cbln4^{N85Q} mice. The fusion RNAs (L7 Transgenes) have higher molecular weights than endogenous L7 which acts as internal standard. The L7-Cbln4 line expressed similar level of mRNA compared to the L7-Cbln1 line. The glycosylation mutant lines (L7-Cbln4^{N26Q} and L7-Cbln4^{N85Q}) expressed lower levels of mRNA compared to L7-Cbln1 and L7-Cbln2 lines previously reported to rescue Cbln1 deficiency (Rong et al., 2012). (d) Cbln4-ir in Purkinje cells of L7-Cbln4 transgenic mice. There is no Cbln4-like ir in cerebellar Purkinje cells of Cbln1 KO mice (i, v). In contrast, there is punctate staining in Purkinje cells of L7-Cbln4 (ii, vi), L7-Cbln4^{N26Q} (iii, vii) and L7-Cbln4^{N85Q} (iv, viii) mice. Note more intense staining in L7-Cbln4 line compared to the two glycosylation mutants. Panel (v), (vi), (vii), (viii) show enlarged views of boxed regions from (i), (ii), (iii), (iv), respectively. Scale bar: 50 μm.

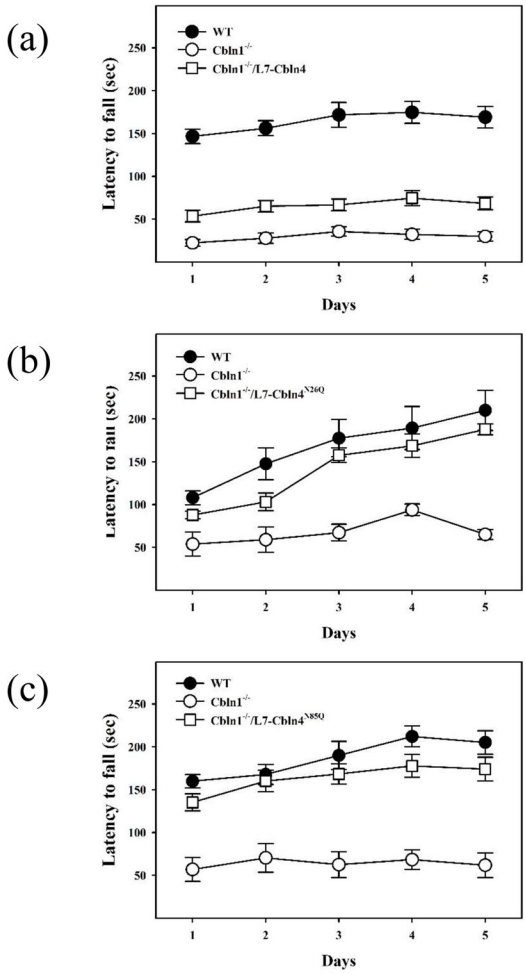

Figure 9.

Ectopic expression of Cbln4, Cbln4^{N26Q} or Cbln4^{N85Q} in Purkinje cells of Cbln1$^{-/-}$ mice improves rotarod performance. The mice (45–55 days, n = 6–8/genotype) were tested on a standardized accelerating rotarod. WT (filled circles) mice, Cbln1$^{-/-}$ (open circles) mice and Cbln1$^{-/-}$ animals carrying a transgene (L7-Cbln4 (a); L7-Cbln4^{N26Q} (b) and L7-Cbln4^{N85Q} (c), open squares) were tested for 5 consecutive days. The latency to fall in seconds was recorded, and data presented as mean ± SEM. Multiple comparisons between groups using the Bonferroni post-hoc test revealed that the presence of L7-Cbln4 (n=6, p<0.01), L7-Cbln4^{N26Q} (n=8, p<0.001), and L7-Cbln4^{N85Q} (n=6, p<0.001), significantly improved the performance of Cbln1$^{-/-}$ animals. The monoglycosylation mutants markedly improved rotarod performance despite their relatively lower level of expression of mRNA and protein compared to L7-Cbln4 [Fig. 8c, 8d].